

Collective excitations and quantum size effects on the surfaces of Pb(111) films: An experimental study

Yade Wang(王亚德), Zijian Lin(林子荐), Siwei Xue(薛思玮), Jiade Li(李佳德), Yi Li(李毅), Xuetao Zhu(朱学涛), and Jiandong Guo(郭建东)

Citation: Chin. Phys. B, 2021, 30 (**7**): 077308. DOI: 10.1088/1674-1056/abfbcd
Journal homepage: http://cpb.iphy.ac.cn; http://iopscience.iop.org/cpb

What follows is a list of articles you may be interested in

Enhanced circular dichroism of TDBC in a metallic hole array structure

Tiantian He(何田田), Qihui Ye(叶起惠), Gang Song(宋钢)
Chin. Phys. B, 2020, 29 (**9**): 097306. DOI: 10.1088/1674-1056/aba9ce

Quantization of electromagnetic modes and angular momentum on plasmonic nanowires

Guodong Zhu(朱国栋), Yangzhe Guo(郭杨喆), Bin Dong(董斌), Yurui Fang(方蔚瑞)
Chin. Phys. B, 2020, 29 (**8**): 087301. DOI: 10.1088/1674-1056/ab9698

Selective excitation of multipolar surface plasmon in a graphene-coated dielectric particle by Laguerre Gaussian beam

Yang Yang(杨阳), Guanghua Zhang(张光华), Xiaoyu Dai(戴小玉)
Chin. Phys. B, 2020, 29 (**5**): 057302. DOI: 10.1088/1674-1056/ab7e97

Strong coupling in silver-molecular J-aggregates-silver structure sandwiched between two dielectric media

Kunwei Pang(庞昆维), Haihong Li(李海红), Gang Song(宋钢), Li Yu(于丽)
Chin. Phys. B, 2019, 28 (**12**): 127301. DOI: 10.1088/1674-1056/ab4fda

Plasmon reflection reveals local electronic properties of natural graphene wrinkles

Runkun Chen(陈闰堃), Cui Yang(杨翠), Yuping Jia(贾玉萍), Liwei Guo(郭丽伟), Jianing Chen(陈佳宁)
Chin. Phys. B, 2019, 28 (**11**): 117302. DOI: 10.1088/1674-1056/ab46a2

RAPID COMMUNICATION

Collective excitations and quantum size effects on the surfaces of Pb(111) films: An experimental study*

Yade Wang(王亚德)[1,2], Zijian Lin(林子荐)[1,2], Siwei Xue(薛思玮)[1,2], Jiade Li(李佳德)[1,2], Yi Li(李毅)[1,2], Xuetao Zhu(朱学涛)[1,2,3,†], and Jiandong Guo(郭建东)[1,2,3,‡]

[1] *Beijing National Laboratory for Condensed Matter Physics and Institute of Physics, Chinese Academy of Sciences, Beijing* 100190, *China*
[2] *School of Physical Sciences, University of Chinese Academy of Sciences, Beijing* 100049, *China*
[3] *Songshan Lake Materials Laboratory, Dongguan* 523808, *China*

(Received 12 April 2021; revised manuscript received 24 April 2021; accepted manuscript online 27 April 2021)

Pb(111) film is a special system that exhibits strong quantum size effects in many electronic properties. The collective excitations, *i.e.*, plasmons, in Pb(111) films are also expected to show signatures of the quantum size effect. Here, using high-resolution electron energy loss spectroscopy, we measured the plasmons on the surface of Pb(111) films with different film thicknesses and analyzed the plasmon dispersions. One surface plasmon branch exhibits prominent damping in the small momentum range, which can be attributed to the interaction between the top and bottom interfaces of the Pb(111) films. With the film thickness increasing, the critical momentum characterizing the damping in Pb(111) films decays not only much slower in Pb(111) films than in other metal films, and even in films with the thickness up to 40 monolayers the damping still exists. The slow decay of the surface plasmon damping, manifesting the strong quantum size effect in Pb(111) films, might be related to the strong nesting of the Fermi surface along the (111) direction.

Keywords: Pb films, plasmons, quantum size effects, high-resolution electron energy loss spectroscopy

PACS: 73.20.Mf, 73.21.–b, 68.49.Jk, 68.47.De **DOI:** 10.1088/1674-1056/abfbcd

1. Introduction

The collective excitations of electrons, *i.e.*, plasmons, in metal films are important not only for the understanding of electron–electron interactions in low-dimensional systems[1,2] but also promising in plasmonic electro-optic applications,[3–11] The properties of plasmons in metal films are mainly determined by the electronic band structure of the metal as well as the dielectric properties of the substrate.[1] The spatial confinement of electrons in the metal films may also generate an essential influence on the plasmon behavior.[12,13] The spatial confinement of metal films in the normal direction will generate the quantization of the electronic states, which can be depicted as the quantum well states (QWS). Due to the discrete energy levels and the electron confinement in the QWS, the properties of metal films, such as the work functions[14] and the transport coefficients,[15] may strongly depend on the thickness, known as the quantum size effect (QSE). The plasmons in metal films sometimes also exhibit obvious QSE, mainly resulting from the inherent QWS. For example, the surface plasmon of Ag films shows negative dispersion in the small momentum range due to enhanced screening effect,[16] and the wave of the QWS can reach the substrate and give rise to the hybridized interaction between the film surface and substrate.[12] Consequently, the damping of the surface plasmon in Ag films displays significant thickness dependence.[17] QSE is a crucial issue to take into account in the research of the surface plasmons of thin films.

A simple classical model, as shown in Fig. 1, is usually used to illustrate the physical picture of the surface plasmons of thin films. When the thin films are grown on the substrate, two interfaces are formed, namely the surface of the films and the interface between the films and the substrate. The coupling between these two interfaces causes the surface plasmon of the film to split into two branches, denoted as ω_+ and ω_-,[18] with $\omega_\pm = (\omega_p/\sqrt{2})\left(1 \pm e^{-qD}\right)^{1/2}$, where ω_p is the bulk plasmon frequency, D is the film thickness, and q represents the parallel momentum. When q exceeding a critical momentum q_c, ω_+ and ω_- converge into one surface plasmon. In some systems, such as the ultrathin Al films on Si(111) substrate,[19] the two split branches are well separated when $q < q_c$ and both of them can be experimentally measured. Yet, in most other cases, *e.g.*, Ag films on Si(111) substrate[17] and Cs films on Si(111) substrate,[20] the splitting cannot be discerned in ex-

*Project supported by the National Natural Science Foundation of China (Grant Nos. 11874404 and 11634016), the National Key Research and Development Program of China (Grant Nos. 2016YFA0302400, 2016YFA0202300, and 2017YFA0303600), and the Strategic Priority Research Program of Chinese Academy of Sciences (Grant No. XDB33000000). Xuetao Zhu was partially supported by the Youth Innovation Promotion Association of Chinese Academy of Sciences.

†Corresponding author. E-mail: xtzhu@iphy.ac.cn
‡Corresponding author. E-mail: jdguo@iphy.ac.cn

© 2021 Chinese Physical Society and IOP Publishing Ltd

periment even when $q < q_c$, since single particle excitations start to dominate the spectrum at small q.[18] In this case, the full width at half maximum (FWHM) of the plasmon increase rapidly when $q < q_c$, originating from the strong damping due to the splitting.[18,21] Figure 1(b) shows the schematic diagram of the plasmon splitting and the corresponding FWHM profile in a thin film. The QSE on the surface plasmons of thin films may be reflected by the change of the critical momentum q_c with film thicknesses.

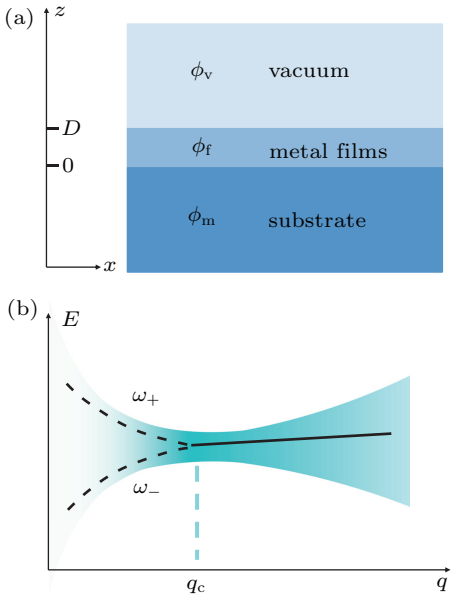


Fig. 1. A classic model of the surface plasmons in thin films. (a) A schematic diagram of the thin film epitaxy on the substrate, showing two interfaces. (b) A schematic plot of the surface plasmon in the film split into $\omega_\pm$ branches. The green background illustrates the change of the width of the plasmon branch, with the q_c defined at the position of the splitting or at the position of the minimum width. The dashed lines of $\omega_\pm$ represent that the splitting may not be experimentally measured.

The most striking metal film system showing the QSE is the Pb(111) film, where the superconducting critical temperature, work function, and the Kondo effect exhibit strong thickness-dependent oscillations.[22–27] Different from other metal films in which the QSE vanishes when the thickness is beyond $\sim$ 10 monolayers (ML),[28–30] the QSE in Pb(111) films is so much stronger that it persists over 30 ML.[24] The plasmons in Pb(111) films are expected to show much stronger QSE than other metal films. However, the manifestation of the strong QSE in the plasmons of Pb(111) films has not been observed so far.

In this article, using high-resolution electron energy loss spectroscopy (HREELS) with the capability of two-dimensional (2D) energy–momentum mapping,[31] we measured and analyzed the plasmon dispersions on the surface of Pb(111) films with different film thicknesses. We discovered that the QSE in Pb(111) films has a very strong effect on one of the surface plasmons, manifested as strong damping in the small momentum range. The damping is still noticeable even in 40-ML-thick Pb(111) films, clearly demonstrating the strong QSE in the perspective of the collective excitations.

2. Methods

The Pb(111) films were grown on the Si(111) 7×7 substrate by molecular beam epitaxy, following the method in Refs. [23,24]. The growth rate was calibrated by the 1/3 ML Pb-induced $\sqrt{3} \times \sqrt{3}$ phase on the Si(111) surface.[32] During the growth, the substrate temperature was maintained at about 150 K by liquid nitrogen cooling. After the film growth, the substrate temperature was slowly increased up to room temperature. In this study, we had grown Pb(111) films with six different thicknesses, *i.e.*, 40, 30, 20, 13, 7, and 4/3 ML, respectively. Low energy electron diffraction and scanning tunneling microscopy were used to characterize the quality of the Pb(111) films, with the results shown in Fig. A1 in Appendix A. HREELS measurements were performed in a spectrometer with the capability of 2D energy–momentum mapping,[31] which provides the energy loss and the scattering angle simultaneously. The momentum transfer $\hbar q$ can be calculated from the scattering angle,[33] according to $\hbar q = \sqrt{2mE_i}\sin\theta_{in} - \sqrt{2m(E_i - E_{loss})}\sin\theta_{sc}$, where θ_{in} and θ_{sc} are the angles of the incident and scattered electron beams, respectively, E_i and E_{loss} are the incident beam energy and loss energy, respectively, and m is the free electron mass. All the HREELS measurements were performed using an incident electron beam with an energy of 110 eV and an incident angle of 60°. Unless otherwise specified, all the HREELS measurements were done at the room temperature. And most of the HREELS measurements were performed along the $\bar{\Gamma}$–$\bar{M}$ direction of the surface Brillouin zone of the Pb(111) films.

3. Results and discussion

As one of the heavy metal elements in the periodical table, Pb possesses large spin–orbit coupling, which may induce topological phases in systems associated with Pb films.[34–37] From theoretical calculations, the spin–orbit effect is also predicted to have a great influence on the plasmons of Pb, *e.g.*, resulting in anisotropy of the plasmons or generating new excitation modes.[38,39] Previous HREELS experiment[40] of Pb(111) films grown on Si(111) focused on a plasmon mode around 2 eV ($q \to 0$), which was assigned to be a surface plasmon. While there was a huge disagreement with the theoretical calculations, where the mode around 2 eV was proved to be a bulk mode related to the spin–orbit coupling of Pb.[38] To clarify the issue, we performed systematical HREELS measurements to show the full dispersions of the plasmons in Pb(111) films and analyzed the possible manifestation of the QSE in the collective excitations.

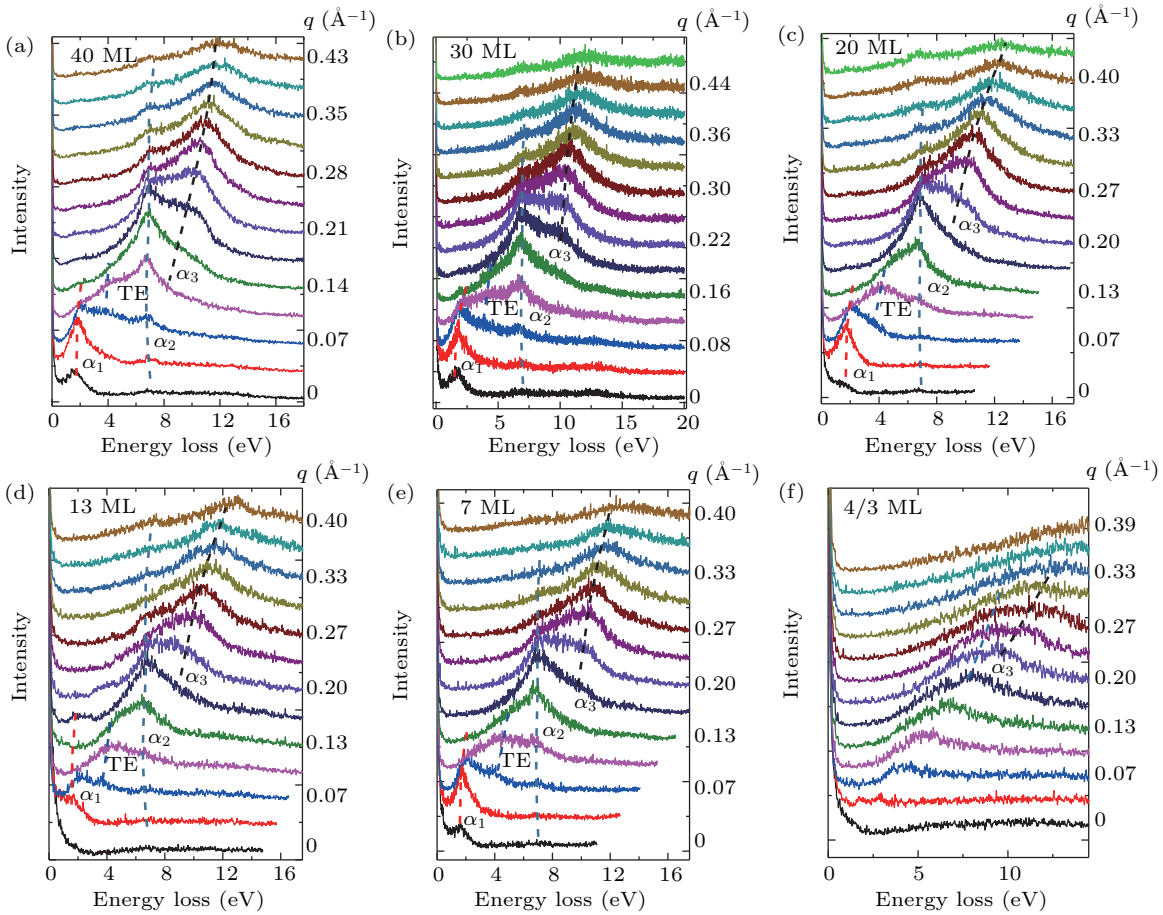


Fig. 2. The momentum-dependent energy loss curves of Pb(111) films with different thicknesses. (a)–(f) corresponding to film thickness of 40, 30, 20, 13, 7, and 4/3 ML, respectively. The dispersions of different branches are represented by dotted lines as guides to the eye.

Figure 2 shows the momentum-dependent energy loss curves (ELCs) of Pb(111) films with different thicknesses, extracted from the 2D HREELS mapping (see Fig. B1 in Appendix B). In the 4/3-ML sample, only two loss peaks can be discerned due to the strong effect of the substrate, since it is actually the Pb-induced reconstruction of the Si(111) surface, with details discussed in the appendix. Except for the 4/3-ML sample, all the other samples show four peaks in the ELCs, marked by the dashed lines and labeled as TE, α_1, α_2, α_3, respectively. In order to check the details about the thickness-dependence, we plot the stacking ELCs of different thicknesses at $q = 0.07$ Å^{-1} and $q = 0.2$ Å^{-1}, in Figs. 3(a) and 3(b), respectively. The line profiles of these modes at different thicknesses are clearly demonstrated. The exact energies of the peaks can be obtained by fitting the ELCs using Lorentz functions. Two typical fitting cases are shown in Figs. 3(c) and 3(d) as examples. The fitting results are plotted in Fig. 4 to show the dispersions of the observed features. The assignments of these features are obtained by comparison with theoretical calculations,[38,41] with the results summarized in Table 1.

Table 1. Summary of the four observed features in the HREELS measurement of the Pb(111) films.

HREELS features	Assignments	Notes
TE	photoemission threshold energy	related to the work function of the film[42,43]
α_1	bulk plasmon	related to the spin–orbit coupling[38]
α_2	surface plasmon	related to interband transitions[41]
α_3	surface plasmon	related to the film thickness[41]

The TE branch represents the photoemission threshold excitation, usually manifested as a single-particle excitation peak in HREELS.[42,43] In Pb(111) films, the TE branch is located at about 4 eV, very close to the work function of Pb (4.25 eV).

The α_1, α_2, α_3 branches are the collective excitations of Pb(111) films. α_1 is a bulk plasmon, with the energy of $\sim$ 1.8 eV at $q = 0$ and dispersing up to $\sim$ 2.1 eV at $q \sim 0.1$ Å^{-1}.

The dispersion matches well (shown in Fig. C1(a) in Appendix C) with the calculated bulk plasmon,[38] which is strongly related to the spin–orbit coupling effect of Pb. α_2 is a surface plasmon, with the energy of ~ 7.0 eV at $q = 0$ and being dispersionless up to $q = 0.4$ Å^{-1}. The comparison with the calculation (shown in Fig. C1(b) in Appendix C) indicates that α_2 is closely related to the interband transitions.[41] The predicted acoustic plasmons in theoretical calculations[38] were not observed in our measurements, possibly because its cross-section, *i.e.*, the intensity in loss functions is too low to show obvious peaks in the ELCs.

α_3 is another surface plasmon, strongly related to the film thickness, which will be the focus in this study. The comparison between α_3 and the calculated surface plasmon dispersion (shown in Fig. C1(b) in Appendix C) indicates that the overall energy of α_3 is slightly lower than the calculated results. This difference should be resulting from the screening effect of the d-electrons, which is difficult to be fully considered in the calculations due to the strong electron–electron interactions. It can be roughly understood by a phenomenological model, where the reduction of the surface plasmon energy due to the additional screening from the d-electrons can be described by Liebsch's theory.[44]

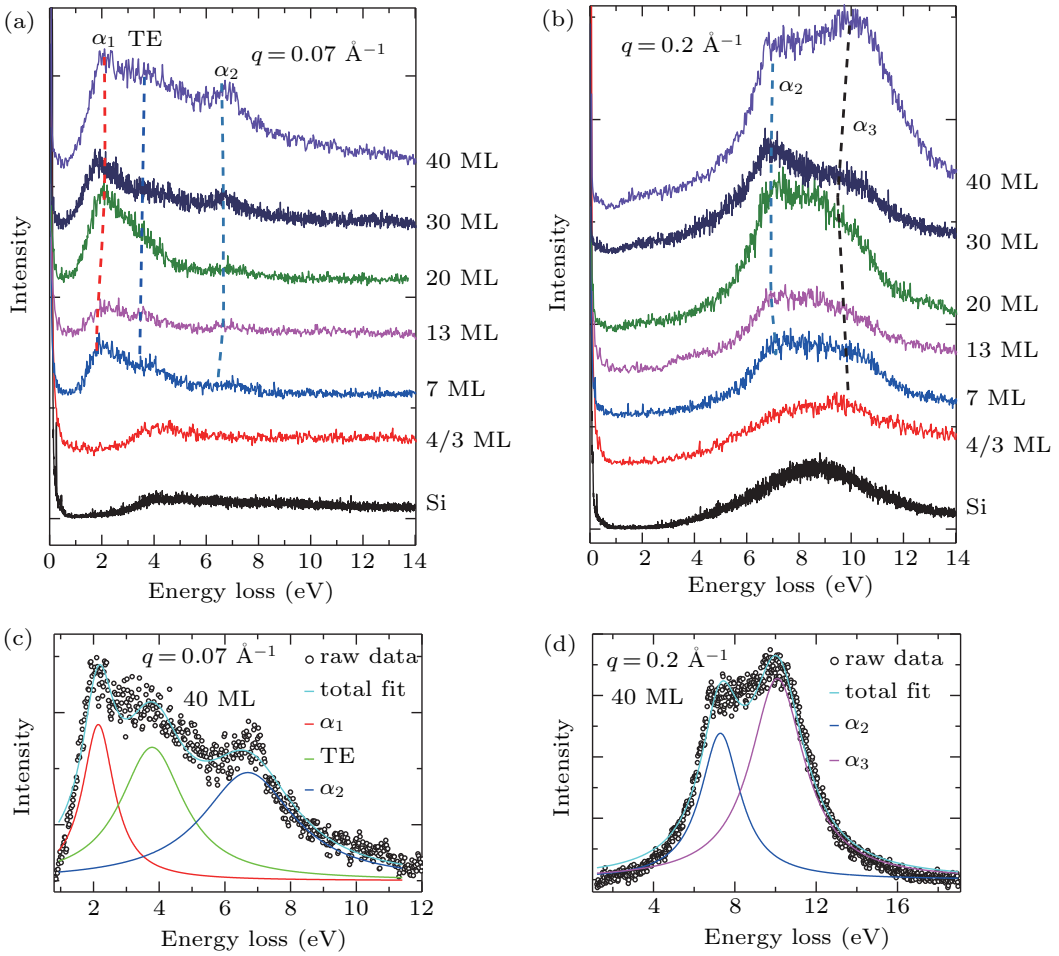


Fig. 3. Comparison of the energy loss curves with different thicknesses and the curve fitting process: (a) the comparison at $q = 0.7$ Å^{-1}; (b) the comparison at $q = 0.2$ Å^{-1}. The dispersion of different branches is represented by dotted lines for guides to the eye; (c) and (d) typical peak fitting process of the 40-ML sample at $q = 0.07$ Å^{-1} and $q = 0.2$ Å^{-1}, respectively.

A prominent feature of α_3 is the damping in the small momentum range, as shown in Figs. 4 and C1(b). In all the films, regardless of the thickness, α_3 cannot be measured around $q = 0$. With increasing q, α_3 gradually appears after the critical momentum value q_c. This phenomenon has not been reported in previous experimental studies of Pb(111) films. There are two possible reasons for the damping of surface plasmons at the small momentum range: (i) the interaction with other collective excitations or (ii) the interaction between the top and bottom interfaces of the thin films.

The first scenario has been reported in two metal film systems, Cs films on Si(111) substrate[20] and Ag films on Cu(111) substrate.[16] In the case of ultrathin Cs films, there is a crossover between the multipole plasmon and the regular surface plasmon.[20] The regular surface plasmon cannot be measured when $q < 0.1$ Å^{-1} due to the influence of the

multipole plasmon.[20] In the case of thin Ag films, the surface plasmon cannot be measured as well when $q < 0.1$ Å^{-1}, where only bulk plasmon can be measured.[16] In both cases, two plasmon modes cannot coexist, *i.e.*, only one mode can be observed at each specific q. As an analogy, in our measurement, it seems α_3 in Pb(111) films at small momentum range could be damped due to the influence of α_2. However, different from the cases of Cs and Ag films, it is clear from Fig. 2 that α_3 and α_2 always coexist when $q > q_c$. These results rule out the possibility that the damping of α_3 at the small momentum range is due to the interaction with other collective excitations.

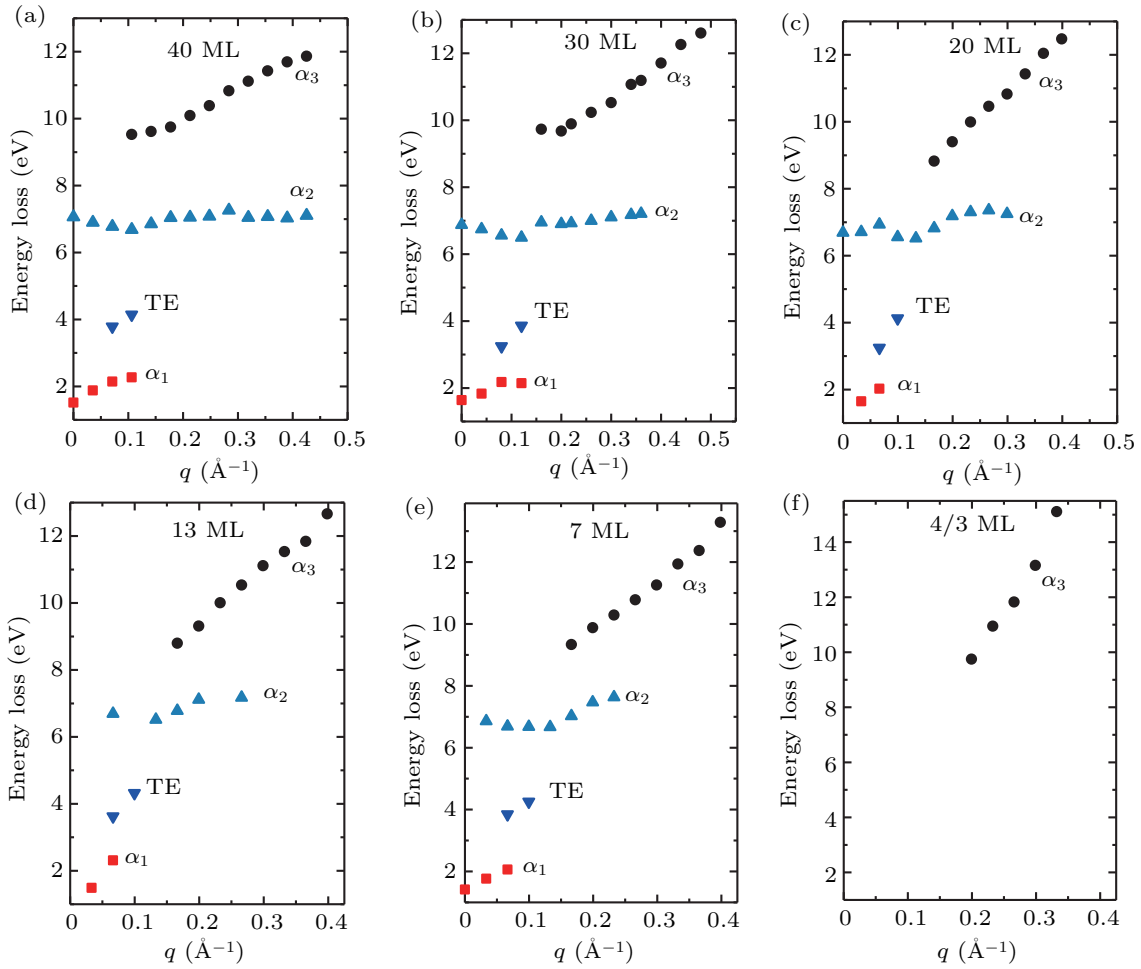


Fig. 4. Dispersions of the measured plasmons obtained from the fitting of loss curves: (a)–(f) corresponding to film thickness of 40, 30, 20, 13, 7, and 4/3 ML, respectively.

The second scenario, *i.e.*, the interaction between the top and bottom interfaces, is essentially a size effect due to the finite film thickness, as illustrated in Fig. 1. This scenario for Pb(111) films has been theoretically calculated in Ref. [41] and the overall damping feature of α_3 observed in our experiment agrees well with this picture. The main difference is that the expected spitting of α_3 in the small momentum range was not clear in the experiment, similar to the case of the surface plasmon in Ag films.[17] Instead, the damping was reflected by the change of the FWHM as a function of q. As described in the scheme of Fig. 1(b), q_c can be determined as the momentum position of the minimum FWHM. To obtain the quantitative value of the q_c for each Pb(111) film with different thickness, the FWHMs of α_3 at different q are obtained from the fitting method shown in Figs. 3(c) and 3(d). The fitting results are plotted in Fig. 5(a). For each thickness, the FWHM gradually decreases with increasing q until reaching the minimum, after which the FWHM starts increasing with q.

As shown in Fig. 5(b), the experimental q_c of Pb(111) is almost maintained around 0.2 Å^{-1} with the film thickness less than 30 ML; and it decays slowly to about 0.15 Å^{-1} when the film thickness is up to 40 ML. The weak and slow decay of the experimentally measured q_c in Pb(111) is significantly different from the case of Ag(111) as well as the calculated of Pb(111), both showing an exponential decay with the increasing film thickness. The observed phenomenon provides a manifestation of the strong QSE in Pb(111) films in the perspective of collective excitations.

The origin of the surprisingly strong QSE in Pb(111) films has been theoretically investigated in Ref. [45]. Com-

pared with other metals, the QSE in Pb(111) films are more prominent due to the slow decay of Friedel oscillations in the electron density from the Pb(111) surfaces, which is related to the strong nesting of the Fermi surface along the Pb(111) direction.[45] The Friedel oscillations at the Pb(111) surface decay as $1/x$ with the distance x from the surface, different from the conventional $1/x^2$ power law at other metal surfaces.[45] Rather than the mere presence of QWS, the interference in the electron density by the strong Friedel oscillations associated with the strong nesting of the Fermi surface along the Pb(111) direction,[45] would inevitably affect the plasmon behaviors. These effects are usually not considered in the *ab initio* calculations, resulting in the possible overestimation of the decay of q_c upon film thickness.[41] The in-depth mechanism of the enhanced interface interactions in the surface plasmons by QSE is still not clear. More studies including both experiments and theories are needed in the future investigations.

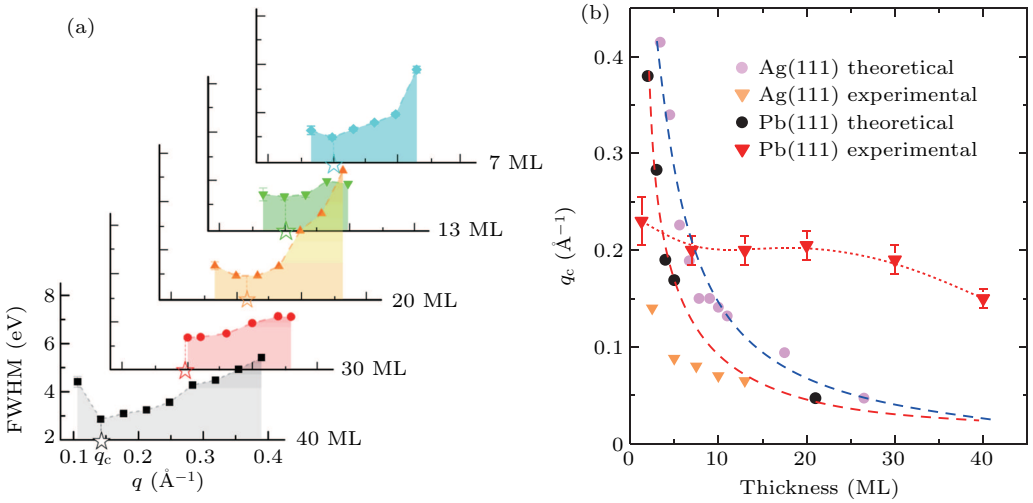


Fig. 5. The critical momentum q_c of different thicknesses: (a) the variation of the FWHW with different film thicknesses of Pb(111). The stars on the horizontal axis mark the positions of the q_c. (b) Comparison of the decay of q_c between different systems. The experimental values of Pb(111) are obtained from panel (a). The theoretical values of Pb(111),[41] experimental values of Ag(111),[17] and theoretical values of Ag(111)[18] are extracted from previous studies.

4. Summary

We have measured the electronic collective excitations in Pb(111) films with different thicknesses. The dispersions of three different plasmons modes have been observed and analyzed. We discovered that one of the surface plasmons shows strong damping in the small momentum range when $q < q_c$, manifesting the strong QSE effect in Pb(111) films. Different from other metal films in which the critical momentum q_c decays exponentially with increasing film thickness, the q_c in Pb(111) films decays much slower, and the strong damping is still observable even in 40-ML-thick Pb(111) films. These observations indicate that the interactions between the surface and interface of the Pb(111) films can be enhanced by the strong Friedel oscillations in the electron density and significantly affect the behaviors of the collective excitations. This work further proves that the QSE is an important issue that should be considered in the analysis of the surface plasmons of thin metal films. Moreover, the thickness-dependent damping behavior originated from the QSE may have potential applications in plasmonics based on metal films.

Acknowledgment

The authors would like to thank Prof. E V Chulkov and Prof. V M Silkin for discussions about the plasmon assignments.

Appendix A: Characterization of the films

The low energy electron diffraction (LEED) patterns of all the Pb(111) films with different thicknesses and the representative scanning tunneling microscopy (STM) images are shown in Fig. A1. These results indicate that the overall surface qualities of the films are good enough to perform the HREELS study. The LEED patterns of the 40- and 30-ML films show clear 1×1 hexagonal Pb(111) spots without any reconstructions. The 20-, 13-, and 7-ML films show some additional fractional spots, which may be related to the reconstructions[23,46] formed during the rising of the substrate temperature from 150 K to room temperature after the growth. The 1-ML Pb coverage is not stable on Si(111) substrate. The thinnest film in this study is with a nominal coverage of 4/3 ML. The 4/3 ML film shows clear $\sqrt{3} \times \sqrt{3}$ reconstruction spots, which corresponds to the striped incommensurate phase as reported previously.[47]

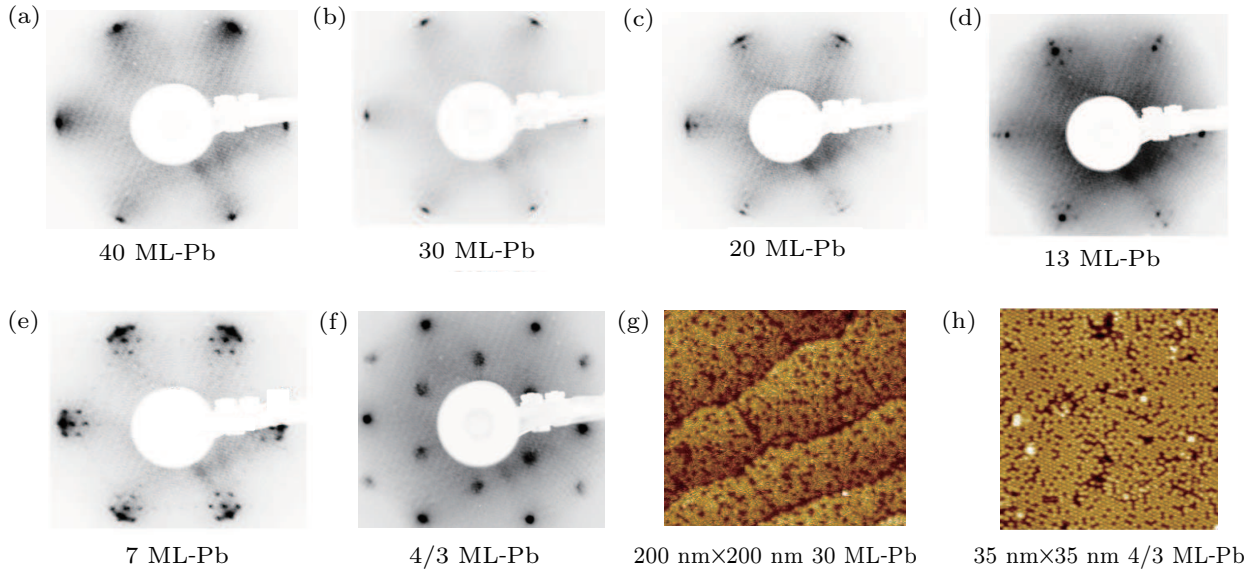


Fig. A1. (a)–(f) The LEED patterns of Pb(111) films with different thicknesses, with the incident electron beam energy of 90 eV. (g) and (h) The STM images ($V = -2$ V, $I = 100$ pA) of 30-ML-thick Pb(111) films and 4/3-ML-thick Pb(111) films, respectively.

Appendix B: Original 2D HREELS data

The original data obtained from our 2D HREELS system are the energy-momentum mappings, as shown in Fig. B1. The momentum-dependent energy loss curves (ELCs), *i.e.*, the scattering intensity as a function of energy loss for a given momentum value, shown in Fig. 2 of the main manuscript, are extracted from these 2D HREELS mappings.

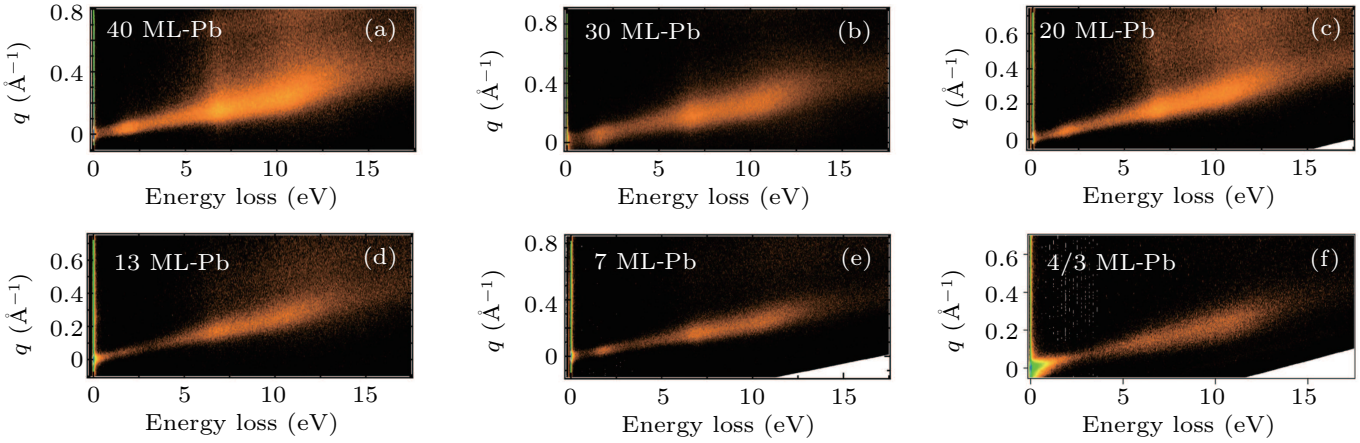


Fig. B1. (a)–(f) 2D HREELS mappings showing the relationship between the energy loss and the momentum of Pb(111) films with different thicknesses.

Appendix C: Comparison of the measured plasmons with theoretical calculations

The assignments of the observed HREELS features are obtained by comparison with theoretical calculations. The colored background in Fig. C1(a) is adopted from the calculated loss functions of bulk Pb,[38] while the colored background in Fig. C1(b) is adopted from the calculated loss functions of Pb(111) films.[41] With our measured energy-momentum points superimposed on the theoretical backgrounds, we can obtain the assignments of the experimentally observed plasmon branches. The results are summarized in Table 1 in the main manuscript. The dispersions of α_1 and α_2 matches well with the calculated results, while the overall energy of α_3 is slightly lower than the calculated results. This difference should be resulting from the screening effect of the d-electrons, which is difficult to be fully captured in the calculations.

In Fig. C1(c), we plot the dispersions of α_3 for the films with different thicknesses in one panel, to show that the overall energy is consistent with the dispersion of the calculated surface plasmon.

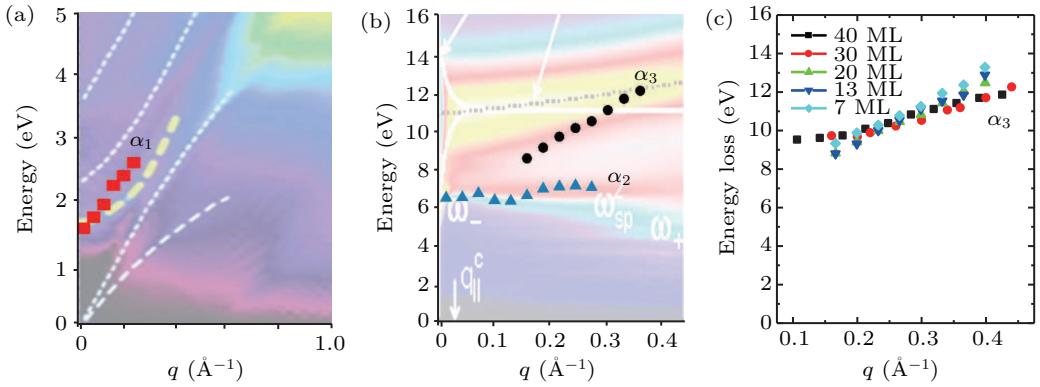


Fig. C1. (a) Comparison of the experimental dispersion (dots) of α_1 (40 ML) with the calculated loss functions (colored background, reprinted by permission from Ref. [38]. Copyright by the American Physical Society.) of bulk Pb. (b) Comparison of the experimental dispersion (dots) of α_2 and α_3 (20 ML) with the calculated loss functions (colored background, reprinted by permission from Ref. [41]. Copyright by the American Physical Society.) of the 21-ML Pb(111) film. (c) The experimental dispersions of the α_3 branch with different thicknesses.

Appendix D: Comparison of the HREELS results between the 4/3-ML-Pb(111) film and Si substrate

As shown in Fig. 2, different from the thicker films in which four energy loss peaks are clearly observed, the 4/3-ML-Pb(111) films can only roughly show two peaks. Especially, the bulk plasmon α_1 can no longer be observed in the ultrathin 4/3-ML-Pb(111) films. Here, in Fig. D1, the HREELS results of the 4/3-ML-Pb(111) films and the Si substrate are compared to show the possible influence from the substrate. It is clear that the ELCs of the 4/3-ML-Pb(111) films are more similar to the substrate than the thicker films, indicating strong substrate effects in the ultrathin films. Similar substrate effects have been previously reported in ultrathin Al films on Si(111).[48] Consequently, the dispersion of theα_3 branch and the corresponding q_c of the 4/3 ML-Pb(111) are not as clear as those of the thick films. The q_c of the 4/3-ML-Pb(111) is roughly estimated from the momentum-dependent ELCs, as shown in Fig. D1(c). All other films with larger thicknesses in our study do not show obvious substrate effects, as shown in Fig. 2.

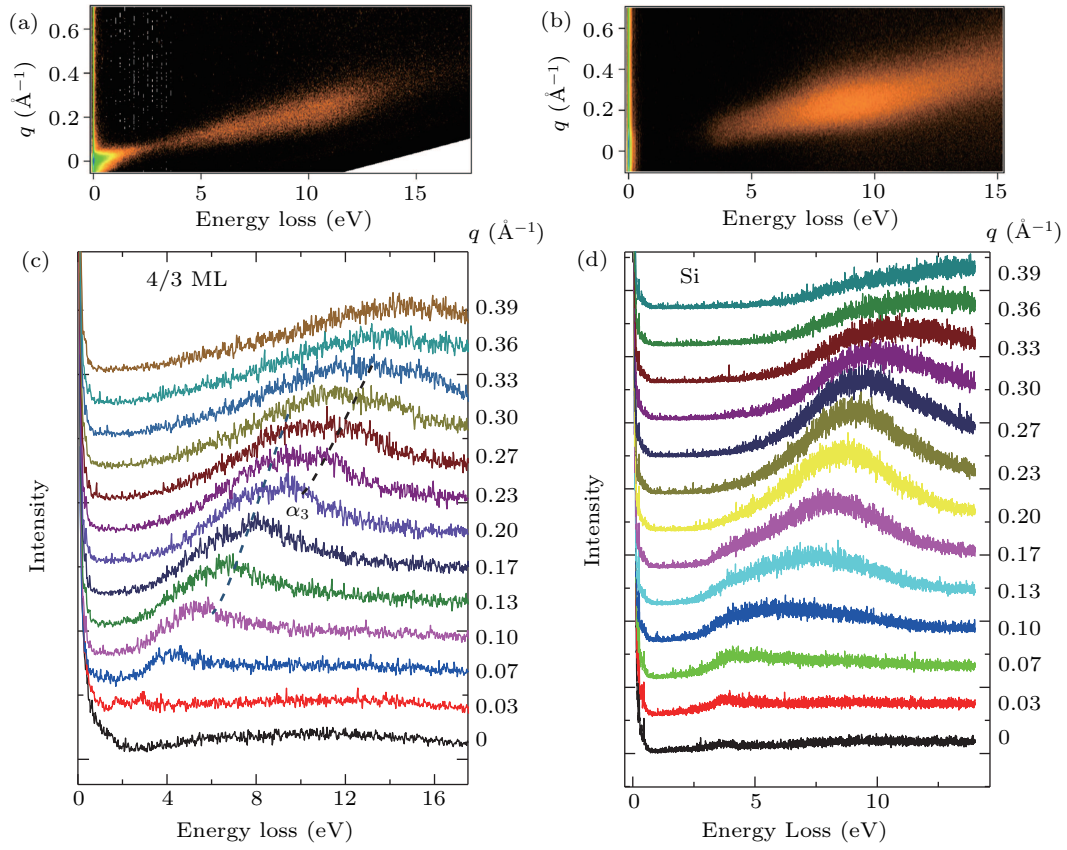


Fig. D1. (a) and (b) The 2D HREELS mappings of 4/3-ML-Pb(111) films and the Si substrate, respectively. (c) and (d) The momentum-dependent ELCs of the 4/3-ML-Pb(111) films and the Si substrate extracted from the 2D HREELS mappings.

Appendix E: HREELS measurements at low temperature

In order to study the influence of temperature on the plasmons of Pb(111) films, we also performed the HREELS measurements on the 30-ML-Pb(111) films at 35 K, with the results shown in Fig. E1. The plasmons of Pb(111) films at 35 K marked in Fig. E1(b) do not show an obvious difference with the results obtained at room temperature.

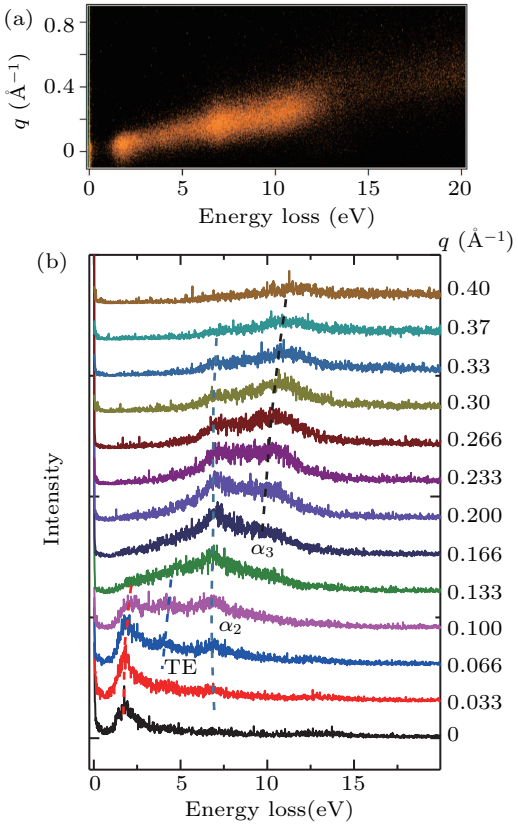


Fig. E1. (a) The 2D HREELS of 30-ML-Pb(111) films measured at 35 K. (b) The corresponding momentum-dependent ELCs.

References

[1] Wang Y, Plummer E W and Kempa K 2011 *Adv. Phys.* **60** 799
[2] Chen R K, Yang C, Jia Y P, Guo L W and Chen J N 2019 *Chin. Phys. B* **28** 117302
[3] Andrew P and Barnes W L 2004 *Science* **306** 1002
[4] Arvind, Vengurlekara S and Ishihara T 2005 *Appl. Phys. Lett.* **87** 091118
[5] Maniyara R A, Rodrigo D, Yu R, Canet-Ferrer J, Ghosh D S, Yongsunthon R, Baker D E, Rezikyan A, Abajo F J G D and Pruneri V 2019 *Nat. Photon.* **13** 328
[6] Suo P F, Mao L and Xu H X 2020 *Chin. Phys. Lett.* **37** 017801
[7] Wang Y L, Zhao B, Min C J, Zhang Y Q, Yang J J, Guo C L and Yuan X C 2020 *Chin. Phys. B* **29** 027302
[8] Peng Z X, Shi Z, Min S H, Quan C Z, Jun Q, Wen X S, Jun Z and Gao D H 2019 *Acta Phys. Sin.* **68** 247301 (in Chinese)
[9] Yang Y, Zhang G H and Dai X Y 2020 *Chin. Phys. B* **29** 057302
[10] Lin W H, Cao E, Zhang L Q, Xu X F, Song Y Z, Liang W J and Sun M T 2018 *Nanoscale* **10** 5482
[11] Cong S, Liu X H, Jiang Y X, Zhang W and Zhao Z G 2020 *The Innovation* **1** 100051
[12] Politano A and Chiarello G 2015 *Prog. Surf. Sci.* **90** 144
[13] Zhao X K, Yuan Y, Lang P L, Guo H L, Shen X, Wang Y G and Yu R C 2016 *Chin. Phys. Lett.* **33** 026802
[14] Feibelman P J and Hamann D R 1984 *Phys. Rev. B* **29** 6463
[15] Trivedi N and Ashcroft N W 1988 *Phys. Rev. B* **38** 12298
[16] Politano A, Formoso V, Colavita E and Chiarello G 2009 *Phys. Rev. B* **79** 045426
[17] Yu Y H, Jiang Y, Tang Z, Guo Q L, Jia J F, Xue Q K, Wu K H and Wang E G 2005 *Phys. Rev. B* **72** 205405
[18] Yuan Z and Gao S W 2006 *Phys. Rev. B* **73** 155411
[19] Qin H J, Jiang Y, Zhang G H and Wu K H 2013 *Appl. Phys. Lett.* **102** 051605
[20] Zielasek V, Rönitz N, Henzler M and Pfnür H 2006 *Phys. Rev. Lett.* **96** 196801
[21] Yuan Z and Gao S W 2008 *Surf. Sci.* **602** 460
[22] Özer M M, Jia Y, Wu B, Zhang Z Y and Weitering H H 2005 *Phys. Rev. B* **72** 113409
[23] Mans A, Dil J H, Ettema A R H F and Weitering H H 2005 *Phys. Rev. B* **72** 155442
[24] Guo Y, Zhang Y F, Bao X Y, Han T Z, Tang Z, Zhang L X, Zhu W G, Wang E G, Niu Q, Qiu Z Q, Jia J F, Zhao Z X and Xue Q K 2004 *Science* **306** 1915
[25] Özer M M, Thompson J R and Weitering H H 2006 *Nat. Phys.* **2** 173
[26] Zhang Y F, Jia J F, Han T Z, Tang Z, Shen Q T, Guo Y, Qiu Z Q and Xue Q K 2005 *Phys. Rev. Lett.* **95** 096802
[27] Fu Y S, Ji S H, Chen X, Ma X C, Wu R, Wang C C, Duan W H, Qiu X H, Sun B, Zhang P, Jia J F and Xue Q K 2007 *Phys. Rev. Lett.* **99** 256601
[28] Zhang Z Y, Niu Q and Shih C K 1998 *Phys. Rev. Lett.* **80** 5381
[29] Wu B and Zhang Z Y 2008 *Phys. Rev. B* **77** 035410
[30] Gavioli L, Kimberlin K R, Tringides M C, Wendelken J F and Zhang Z Y 1999 *Phys. Rev. Lett.* **82** 129
[31] Zhu X T, Cao Y W, Zhang S Y, Jia X, Guo Q L, Yang F, Zhu L F, Zhang J D, Plummer E W and Guo J D 2015 *Rev. Sci. Instrum.* **86** 083902
[32] Ganz E, Hwang I S, Xiong F L, Theiss S K and Golovchenko J 1991 *Surf. Sci.* **257** 259
[33] Ibach and Mills D L 1982 *Electron energy loss spectroscopy and surface vibrations* (New York: Academic) p. 1
[34] Li Y, Zhang J Y, Zhao B, Xue Y and Yang Z Q 2019 *Phys. Rev. B* **99** 195402
[35] Yu X L, Huang L and Wu J S 2017 *Phys. Rev. B* **95** 125113
[36] Sassmannshausen J, Kubetzka A, Hsu P J, Bergmann K V and Wiesendanger R 2018 *Phys. Rev. B* **98** 144443
[37] Bihlmayer G, Sassmannshausen J, Kubetzka A, Blügel S, Bergmann K V and Wiesendanger R 2020 *Phys. Rev. Lett.* **124** 126401
[38] Zubizarreta X, Silkin V M and Chulkov E V 2013 *Phys. Rev. B* **87** 115112
[39] Zubizarreta X, Silkin V M and Chulkov E V 2014 *Phys. Rev. B* **90** 165121
[40] Teng A 2014 *Quantum Tuning of Plasmons in Ultrathin Metal Films*, Ph. D. Dissertation (Knoxville: University of Tennessee)
[41] Zubizarreta X, Chulkov E V, Chernov I P, Vasenko A S, Aldazabal I and Silkin V M 2017 *Phys. Rev. B* **95** 235405
[42] Teng A, Kempa K, Özer M M, Hus S M, Snijders P C, Lee G and Weitering H H 2014 *Phys. Rev. B* **90** 115416
[43] Liebsch A 1987 *Phys. Rev. B* **36** 7378
[44] Liebsch A 1997 *Elementary Excitation on Metal Surfaces* (New York: Plenum) p. 92
[45] Jia Y, Wu B, Li C, Einstein T L, Weitering H H and Zhang Z Y 2010 *Phys. Rev. Lett.* **105** 066101
[46] Yakes M and Tringides M C 2011 *J. Phys. Chem. A* **115** 7096
[47] Seehofer L, Falkenberg G, Daboul D and Johnson R L 1995 *Phys. Rev. B* **51** 13503
[48] Yuan Z, Jiang Y, Gao Y, Käll M and Gao S W 2011 *Phys. Rev. B* **83** 165452